2008 IEEE International Conference on
Robotics and Automation
Pasadena, CA, USA, May 19-23, 2008

Physiological Motion Rejection in Flexible Endoscopy using Visual Servoing

L. Ott*, Ph. Zanne, Fl. Nageotte, M. de Mathelin and J. Gangloff
{lott,zanne,nageotte,demath,jacques}@eavr.u-strasbg.fr

Abstract— **Flexible endoscopes are used in many surgical procedures and diagnostic exams, like in gastroscopy or coloscopy. They have also been used recently for new surgical procedures using natural orifices called NOTES. While these procedures are very promising for the patients, they are quite awkward for the surgeons. The flexible endoscope allows the access to operating areas which are not easily reachable, with small or no incisions; but the manipulation of the system is complex. In order to help the practicians during NOTES or classical interventions with flexible endoscopes, we propose to motorize the system so as to partially robotize the movements. This paper presents the problems in the use of the flexible endoscope and explains how the system can be used to stabilize the endoscope on an area of interest despite physiological motions and therefore to improve the manipulation of the system.**

I. INTRODUCTION

A new surgical technique called NOTES (Natural Orifice Transluminal Endoscopic Surgery) [1] is currently under development on the animal model, and at the stage of the first trials on human beings. It consists of accessing the peritoneal cavity by passing through a natural orifice (such as the mouth and then the esophagus, or the anus and then the colon) and then to make an opening in an inner wall (such as the stomach wall) to accomplish treatments such as cholecysectomies [2]. On April 2nd 2007, the first human no-scar operation was carried out using a flexible endoscope for transvaginal cholecystectomy on a 30-year-old woman with symptomatic gallstones at the University Hospital of Strasbourg by Professor Jacques Marescaux and his team [3].

The main advantage of this new surgical technique is to avoid incisions in the abdominal wall for passing the instruments. Incisions made in inner walls heal faster than those made in the abdominal walls. As a consequence, patients will have less post-operatory traumas, and the absence of wound on the patient body will have a positive psychological effect.

The material currently used to perform these procedures is conventional material from gastroenterology. These instruments are not completely well suited for this new technique and new tools are currently under development. A solution to assist the surgeons during these operations is to partly robotize the movement of the endoscope so as to automatically follow the motions of the organs of interest.

Physiological motion compensation using robots is a very promising approach for assisting surgeon in difficult operations [4]. This has been used in laparoscopic surgery for compensating the breathing motion [5] and in cardiac surgery for stabilizing the surgical instruments with respect to the beating heart [6].

But to our knowledge, physiological motion rejection has never been carried out using flexible endoscopes. The main differences arise from the difficulty to obtain a kinematic model for these flexible systems and from the backlashes in the wire transmission. Moreover, the camera is embedded in the endoscope in an eye-in-hand configuration. The consequence is that physiological motions and self-motion of the endoscope can hardly be separated.

We present two control algorithms for physiological motion compensation, a repetitive controller and a generalized predictive controller (GPC), and we study the behaviour of the control loop in disturbance rejection and with respect to reference modification. These algorithms have been tested on a laboratory setup and *in vivo* on a porcine model.

The paper is organized as follows : The second section presents the problematic of this work. Section III presents the mechanical and vision model of the flexible endoscopic system. The proposed control algorithms for periodical motion rejection are presented in section IV. Finally, simulations and *In vivo* results are given and discussed in section V.

II. MOTIVATIONS

A. Conventional endoscopes

Conventional flexible endoscopes used in gastroenterology generally consist in three parts (Figure 1) : A control handle with two navigation wheels, a flexible shaft usually more than one meter long with a circular cross section, and a distal bending tip about 10 cm long. In order to navigate inside the human body, to control the trajectory of the flexible endoscope or to guide the instruments, the practician uses the images transmitted by an optical system (CCD camera), embedded at the tip of the endoscope.

The angle of the tip deflection is controlled by pull-wires running all the way through the endoscope shaft to the navigation wheels. The endoscope tip can bend along two orthogonal directions. The illumination of the body cavity is provided by an optical fiber going through the flexible endoscope. One or several working channels allow the transit of endoscopic tools. Once on the operating site, the surgeon can use tools such as scissors, hooks, bistouris, forceps, or needles depending on the operation to be performed and switch them without modifying the position of the endoscope.

Authors are with LSIIT (UMR CNRS-ULP 7005), Strasbourg I University, France.

Authors would like to thank *Karl Storz GmbH* for their support.
*This work is supported by a grant from the Alsace Regional Council.

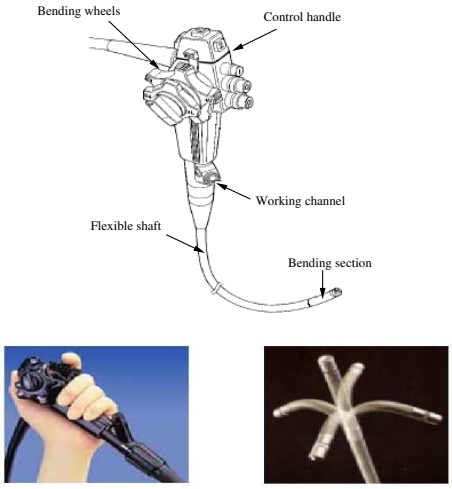

Fig. 1. Basic components of a flexible endoscope

B. Problematic of flexible endoscope manipulation

The surgeon faces numerous challenges when handling flexible endoscopes since he has to combine various actions to perform the desired movements. The possible actions are the rotation of the wheels, the forward/backward motion of the endoscope and the rotation of the endoscope. The shape of the flexible shaft being unknown, the handlings upon the endoscope body have unpredictable effects in the endoscopic image. Although the rotation of the wheels have a known effect, it is not intuitive and requires training. Physiological motions of the organs (breathing) and motions of the patient generate critical disturbances on the flexible endoscope. To operate despite these disturbances requires an expert hand-eye coordination.

Moreover, the classical endoscopic tools are not articulated. The surgeon can only push or pull them inside the endoscope, which results in a translation along the direction of the endoscope's tip. Thus, it is not possible with the existing multi-channel endoscopes to give independent off-axis motion to each tool.

For instance, in transluminal operations, several practicians must handle simultaneously the endoscopic device because of the high number of mobility to manage. They hence have to share a small working space around the endoscope control handle, and to demonstrate a good coordination.

III. ROBOTIC ASSISTANCE

A. Objectives

In order to supply a robotic assistance to the praticians during flexible endoscopy interventions, we have developed an automated positioning system of the endoscope tip. The objective is to realize a virtual link between the tip of the endoscope and an anatomical target despite the physiological motions, the interaction of the instruments with the environment and the manually controlled forward/backward motion of the endoscope. The pratician can thereby focus on the manipulation of the endoscopic tools while the bending section compensate the occurring disturbances. The virtual link between the tip and the anatomical target is performed using a 2D visual servoing scheme in association with the selection of relevant visual features.

B. Endoscope motorization

Our robotic endoscope prototype is based on a single working channel flexible gastroscope *Karl Storz 13801PKS*. The navigation wheels have been replaced by two hollow shaft rotary motors (*Harmonic Drive FHA-8C*) which drive two coaxial shafts coming out from the handle. Each shaft is connected to one wire loop in the handle. By using hollow shaft motors, it has been made possible to drive the two coaxial shafts without adding gears in the assembly. In this way, we do not add additional backlashes to the system. The motors are controlled using velocity loop servo controller *Harmonic Drive SC-610*.

We denote $Q = [q_1, q_2]^T$ the vector of the joints positions of the motors and $\dot{Q} = [\dot{q_1}, \dot{q_2}]^T$ the joint velocities. J_q is the Jacobian of the mechanical system which maps the joint velocities to the cartesian velocity of the head of the endoscope. The kinematic model of the system is difficult to obtain as the position of the wire inside the body of the endoscope is unknown. However, the instantaneous velocity of the endoscopic camera is mainly a translation in the image plane denoted by v_x, v_y. Hence J_q is a 2×2 matrix.

C. Backlashes non linearity

Flexible endoscopes have a complex non linear behaviour. The wire transmission between the navigation wheels and the bending section induces backlashes. Furthermore, the deadbands of these backlashes depend on the configuration of the flexible endoscope. Fig 2 and 3 show the position of a static target during forth-and-back rotations of the motors. In Fig 2, the endoscope bending section is straight, while in Fig 3 it is curved at 90°. As the deadband of these backlashes depends on the configuration, we cannot identify the deadband size and apply the corresponding backlash inverse model. An on-line estimation of the backlashes deadbands is required. Tao and Kokotovic [7] present an adaptive inverse backlash compensation, but the output of the system needs to be observable. In our case, the output measure is the target position in the image plane, but it is subject to breathing disturbance. In this paper, we do not cover the backlash compensation problem.

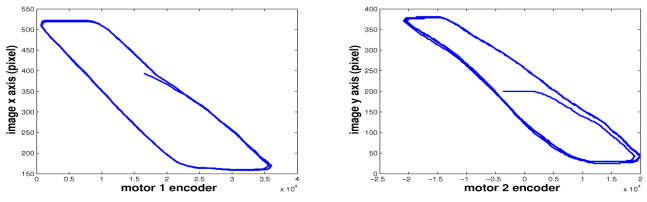

Fig. 2. Backlashes hysteresis for axis 1 (left) and 2 (right) in an extended configuration

D. Visual feedback

The video output of the endoscopic system is a standard PAL video signal. Hence the sampling frequency of the

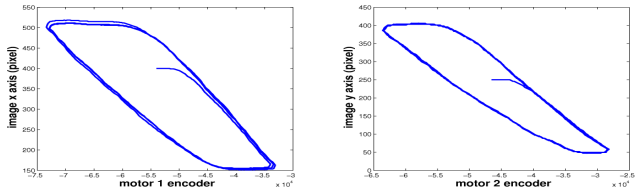

Fig. 3. Backlashes hysteresis in a bent configuration

vision loop is 25 Hz ($T_s = 0.04s$). Since the mechanical system has only 2 DOFs, the two coordinates of a visual feature in the image $F = [u, v]^T$ (for example a point) is a sufficient feedback variable to control the system (see section V-C for more details on the feature extraction).

The velocity of the image feature $\dot{F}$ is related to the joint velocity $\dot{Q}$ by the interaction matrix denoted J [8]. For the considered system, the interaction matrix is a 2×2 matrix which can be decomposed the following way : $J = J_{im} J_q$ where J_{im} is the image Jacobian which maps the velocity screw of the camera $[v_x, v_y]$ to the velocity of the image features. The analytical expression of J_{im} is simply given by

$$J_{im} = \begin{bmatrix} \frac{k_u}{L} & 0 \\ 0 & \frac{k_v}{L} \end{bmatrix}$$

where k_u and k_v are the magnifying factors of the camera along each direction. It also depends on the depth L of the feature with respect to the camera.

In many applications of visual servoing, it is possible to estimate the depth, either by using knowledge on the structure of the feature, or by using multiple views. Both techniques assume that the object of interest is rigid. Unfortunately, this is not the case for the aimed application, since organs deform under physiological motions. As a consequence the depth cannot be easily estimated. Since the jacobian J_q is also unknown, we chose to directly estimate J in a preliminary stage around the working configuration (see section V-E for more details).

E. Model of the visual loop

The model of the visual loop is given in Figure 4. The joint velocity vector $\dot{Q}^*$ will be sent as reference to the built-in velocity loops of the joints power amplifiers. The bandwidth of the joints velocity loops being largely higher than the sampling frequency of the visual loop, the dynamic of the actuators can be neglected and we have $\dot{Q} \sim \dot{Q}^*$.

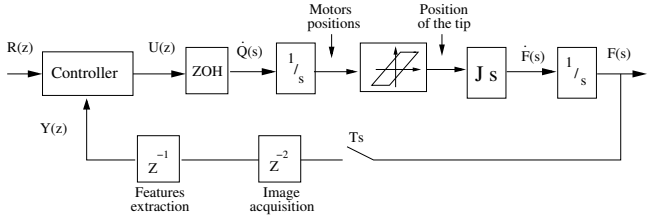

Fig. 4. block diagram of the visual servoing loop

The discrete time transfer function between the velocity and the position of the features in the image is then given by

$$G(z) = \frac{Y(z)}{U(z)} = z^{-3}(1 - z^{-1})\mathscr{Z}\left\{\frac{J}{s^2}\right\} = J\frac{T_s \cdot z^{-4}}{1 - z^{-1}}$$

where $\mathscr{Z}$ represents the z-transform. The delay z^{-3} in the feedback loop is used to take into account the image acquisition and processing time.

IV. PERIODIC MOTIONS CANCELLATION

During a transluminal intervention, the patient is anesthetized and placed under artificial ventilation. Since the respiration is mechanically forced, its cycle is perfectly periodical. We present here two types of control algorithm which can be used to reject unknown periodic disturbances. Their performances for periodic disturbances rejection is presented as well as their behaviour with respect to reference shifts and their robustness with respect to errors on the model.

A. Repetitive control

The concept of repetitive control has been initiated by Inoue et al. [9] for high accuracy tracking of a periodic reference with a known period. We use here the repetitive controller known as prototype repetitive controller [10]. This method features a controller consisting of a periodic signal generator and an approximate inverse of the system. For a stable minimum phase system

$$P(z^{-1}) = z^{-d}\frac{B(z^{-1})}{A(z^{-1})}$$

the prototype controller is given by

$$C_r(z^{-1}) = K_r \frac{z^{-N+d} A(z^{-1})}{B(z^{-1})} \cdot \frac{1}{1 - z^{-N}} \qquad (1)$$

where $K_r \in]0, 2]$ is the repetitive control gain, and N is the number of sampling periods in one period of the disturbance. In particular, when $K_r = 1$, null tracking error can theoretically be obtained after one perturbation period.

Repetitive control has been formalized for SISO system. In our case, the mechanical construction of the endoscope is such that the interaction matrix exhibits little coupling. Thus, a separate servo loop can be implemented for each actuator. Let J_x be the term of the Jacobian matrix giving the relation between the u image coordinate and the first actuator with joint position q_1. The SISO model for the visual servo loop becomes

$$G_x(z^{-1}) = J_x \frac{T_s \cdot z^{-4}}{1 - z^{-1}}$$

This system is not stable, but it is possible to use the same formalism as in Eq.1 because the signal generator contains a pole in 1. The associated repetitive controller is then

$$Cr_x(z^{-1}) = K_r \frac{\hat{G}_x^{-1}(z^{-1}) \cdot z^{-N}}{1 - Q(z, z^{-1}) \cdot z^{-N}}$$

where $Q(z,z^{-1})$ is a zero phase shift unity gain low-pass filter, for instance $Q(z,z^{-1}) = 0.1 \cdot z^2 + 0.15 \cdot z^1 + 0.5 + 0.15 \cdot z^{-1} + 0.1 \cdot z^{-2}$. It limits the gain of the controller at the high frequency harmonics of the perturbation and hence increase the robustness of the control loop with respect to noises.

B. R-GPC

In the context of surgical robotic, the system must be able to correctly react to references changes. This is especially important in our application since the endoscopic tools are not articulated and the endoscope must be moved to reach different points of interest. Hence the system should be able to fulfill both following objectives : output periodic disturbances must be rejected and the surgeon should be able to control the position of the head on the virtually stabilized environment. Gangloff et al. [5] proposed a modified version of the Generalized Predictive Controller called R-GPC. In the R-GPC formulation, the reference following function is clearly separated from the periodical disturbance rejection.

The classical GPC is a model predictive controller which computes at each step the control input to be sent to the system so as to minimize a cost function on a given time window. Only the first control input is then actually sent to the system. For this purpose, a repetitive ARIMAX model of the system is used

$$A(q^{-1})y(t) = B(q^{-1})u(t-1) + \frac{C(q^{-1})}{\Delta(q^{-1})}\xi(t)$$

where q^{-1} is the backward operator, A and B are two polynomials modeling the system dynamics. $\xi(t)$ is a zero-mean white noise colored by polynomial C and made non-stationary by polynomial Δ.

$$\Delta(q^{-1}) = 1 - Q(q^{-1},q)q^{-N}$$

allows to model periodic disturbances, where $Q(q^{-1},q)$ as defined before, is used for stabilizing purposes.

Classically the cost functions depend on the predicted error and on the control energy and have the following form

$$J(u,t) = \sum_{j=N_1}^{N_2} \|\hat{y}_{\mathtt{th}}(t+j) - r(t+j)\|^2 + \lambda \sum_{j=1}^{N_u} \|\delta u(t+j-1)\|^2$$

where δu are the control input increments, $r(t)$ is the reference signal, N_1, N_2 are the bounds of the prediction cost horizon and N_u is the length of the control cost horizon, λ weights the control energy.

The principle of the R-GPC is presented on Fig 5. gpc1 is used to compute the control input $u_1(t)$ which should ensures reference tracking, while gpc2 is used to minimize the error between the measure and the output predicted by gpc1, and hence disturbance rejection. It clearly appears that if the model of the system is accurate, then the entry of gpc2 does not contain the effects of the reference changes. Therefore, these changes are not anymore considered as a periodical disturbance.

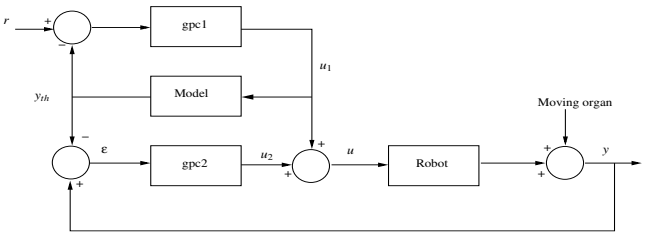

Fig. 5. R-GPC bloc diagram

The overall cost function of the R-GPC is :

$$J(u = u_1 + u_2, t) = \sum_{j=N_1}^{N_2} \|\hat{y}_{\mathtt{th}}(t+j) - r(t+j)\|^2 + \sum_{j=N_1}^{N_2} \|\hat{\varepsilon}(t+j)\|^2 + \lambda \sum_{j=1}^{N_u} \|\delta u_1(t+j-1)\|^2 + \mu \sum_{j=1}^{N_u} \|\delta u_2(t+j-1)\|^2$$

where λ and μ weight the control energies respectively for reference tracking and disturbance rejection.

Details of the computation of this control law can be found in [5].

V. RESULTS

A. Simulations

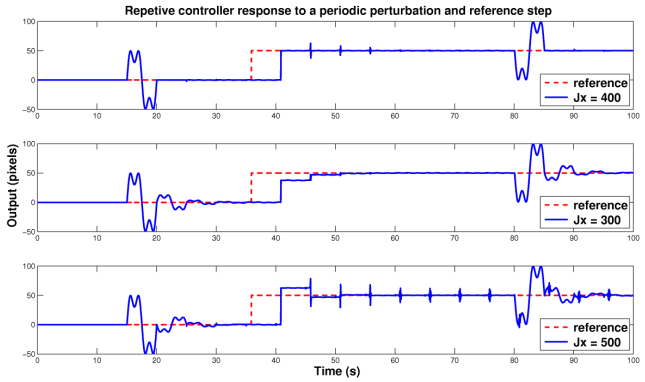

Fig. 6. Repetitive controller response to a periodic disturbance and a reference step

The Repetitive controller and R-GPC have both been tested in simulation on a SISO model. The model used to build the controllers is $\hat{G}_x(z^{-1}) = \hat{J}_x \cdot \frac{T_s \cdot z^{-4}}{1 - z^{-1}}$ with $\hat{J}_x = 400$, $T_s = 0.04s$. Fig 6 and Fig 7, show the responses of the closed loop with a periodic disturbance on the output and a reference changes at time $t = 36s$ respectively for the Repetitive and R-GPC controllers. The disturbance fundamental frequency is 0.2 Hz. The periodic disturbance appears at time $t = 15s$ and disappears at $t = 80s$.

Since the interaction matrix has to be estimated in our experiments, we have simulated the effect of estimation errors on $\hat{J}_x$ with both controllers.

The Repetitive controller gain K_r is set to 1.0. For the R-GPC, the polynomial C is chosen as $C = 1 - z^{-1}$, the other

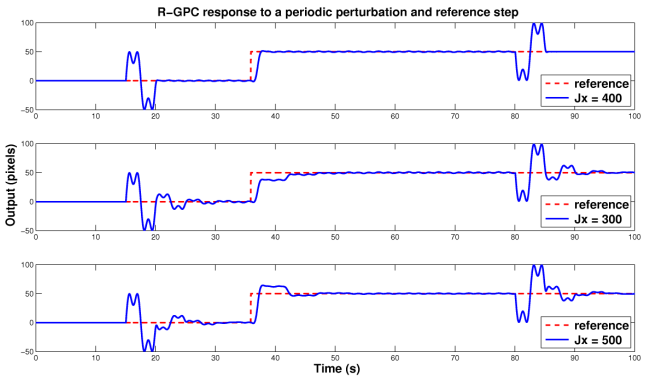

Fig. 7. R-GPC controller response to a periodic disturbance and a reference step

parameters are chosen as $N_1 = 4$, $N_2 = 30$, $N_u = 30$, $\lambda = 500000$, and $\mu = 10000$.

B. Discussion

For our system, both repetitive and R-GPC controllers exhibit overshoot when the gains of the model are underestimated. On the contrary, the reference is not reached during the first disturbance period when gains are overestimated. Both effects are then corrected during the subsequent periods. The control loop is stable as long as the estimated gains are greater than half the real gains. In this limit case, the overshoot is one hundred percent and the systems begins to oscillate.

Fig 6 shows that, with the repetitive controller, the reference change is followed by sudden motions of the output especially when gains are underestimated. A fast, non periodical variation of the reference yields an error which is learned and considered as periodical by the controller. In the subsequent period, the controller tries to anticipate a variation of the reference that does not occur. This yields a peak on the output that is repeated periodically and attenuated over time. The R-GPC controller is better for reference tracking as the reference is considered separately and hence not considered as a periodical disturbance.

The behaviour of the repetitive controller is then globally better for overestimated gains than for underestimated ones, whereas the behaviour of the R-GPC is comparable for under and over-estimated gains, as long as the stability is guaranteed.

C. Visual features

The selection and tracking of relevant visual features in the development of a visual servoing scheme are primary concerns. Contrary to classical problems where the environment is rigid, well structured, or artificially marked, the environment of our application is complex without the possibility to add fiducials.

In the laboratory and *in vivo* experiments, the visual features F are the coordinates of the center of a window, first defined by the user, and tracked using either the Mean Shift algorithm [11], or the ESM tracking algorithm [12].

D. Laboratory Test Bed

We have developed a testbed to validate the control strategy in our laboratory before making in vivo experiments. We use a model of abdominal cavity organs to simulate the real environment. This model is fixed to a motorized device, so that the motion of the target can be precisely controlled to make a perfectly periodic displacement. The motorized endoscope is statically fixed to the table and the only disturbance is due to the moving target. These experiments have been carried out using accurately estimated gains on the non-moving target.

Figure 8 and 9 show that several periods are actually required to correctly learn the perturbation. This is due to the backlashes in the system which have not been taken into account into the model of the system. Despite these backlashes, the error converges towards zero and the image is perfectly stabilized.

Similarly, figure 9 shows that the reference change is also correctly tracked after several periods. The reference is not reached during the first period because of backlashes which absorb a part of the control input energy. These results plead for underestimating gains.

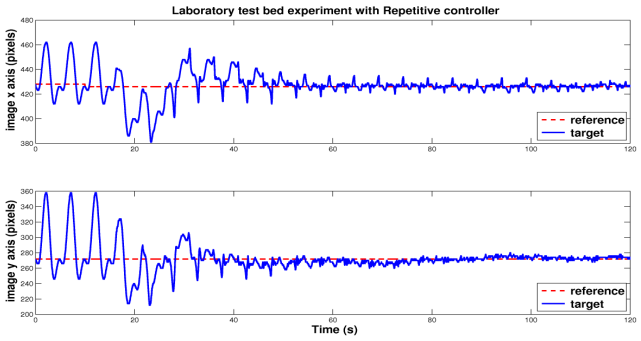

Fig. 8. Laboratory test bed experiment with the repetitive controller. top : x axis of the image, bottom : y axis. The controller is activated at t=10s.

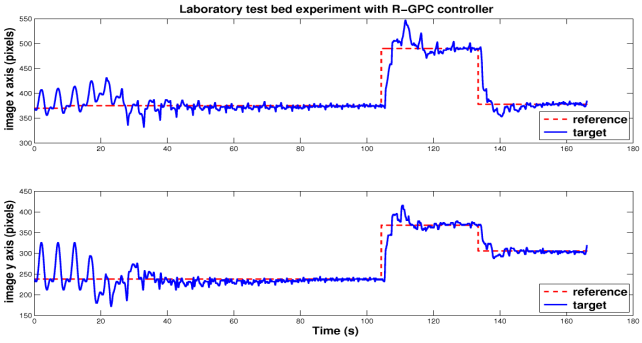

Fig. 9. Laboratory test bed experiment with the R-GPC controller. top : x axis of the image, bottom : y axis. The controller is activated at t=10s and a new reference arrives at t=105s.

Fig. 10. Left, image acquired by the flexible endoscope camera. Right, external view acquired by a laparoscope

E. In Vivo experiments

We have performed experiments[1] on an anesthetized pig placed under artificial ventilation. The controlled bending section of the motorized endoscope was inserted in the abdominal cavity by passing through a trocar. We chose to focus our experiments on the liver (see Fig 10) which is subject to large respiration motion. The image target is a burn onto the organ which is tracked using the Mean-Shift algorithm. Note that in this experiment, as the endoscope is constraint in the trocar, the breathing motion acts not only on the moving target, but also on the flexible shaft of the endoscope. Gains estimates are easily tuned manually by a test and try procedure by first using high gains which guarantee stability. Results are presented on figures 11 and 12.

The control algorithms allow to reduce the amplitude of the motion of the feature by factor four in less than 20 seconds. The R-GPC also allows to track the changing reference with a good accuracy. The amplitude of the remaining motion is larger than for laboratory experiments because of the noise on the position of the image feature. The quality of the stabilization has been acknowledged by our medical partners.

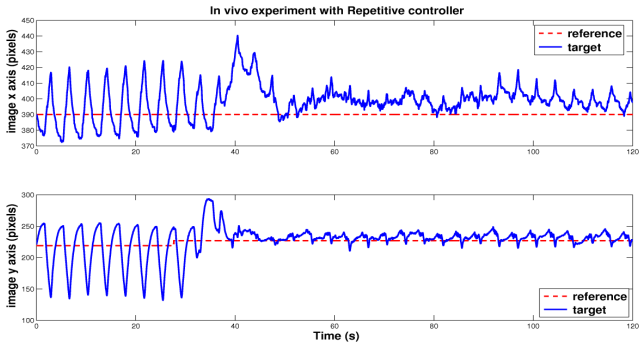

Fig. 11. In vivo experiment with the repetitive controller. The controller has been activated at t=30s.

VI. CONCLUSIONS

We have shown in this paper that it is possible to control a flexible endoscope for breathing compensation using only the embedded vision system of the endoscope. *In vivo* experiments exhibit very promising results. Both control algorithms, repetitive and R-GPC, have satisfying behaviour

[1]See the video at ftp://eavr.u-strasbg.fr/pub/laurent/respendoflex.avi

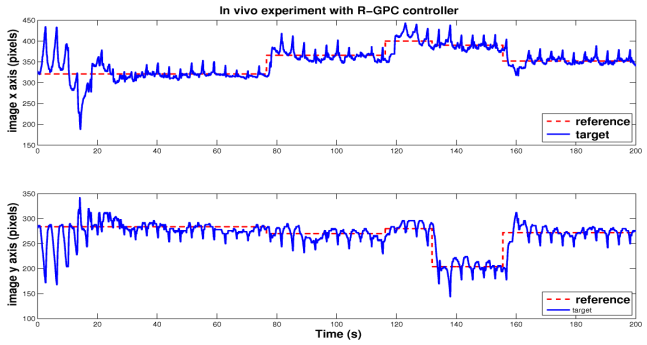

Fig. 12. In vivo experiment with R-GPC controller. The controller has been activated at t=10s. Several references changes have been applied along x and y axes of the image.

according to the surgeons who have assessed the system at the IRCAD - Strasbourg. The proposed approach can be used for stabilizing the endoscopic view in transluminal operations and hence decrease the number of surgeons manipulating the system. There are also other possible applications in classical gastroscopy for example for stabilizing the endoscopic view during tumor resection.

REFERENCES

[1] C.W. Ko, A.N. Kalloo, Per-oral transgastric abdominal surgery, *Chinese Journal of Digestive Diseases*, 2006, 7 : 67-70

[2] P.O. Park, M. Bergström, K. Kikeda et al, Experimental studies of transgastric gallbladder surgery : cholecystectomy and cholecystogastric anastomosis, *Gastrointestinal Endoscopy*, 2005, 61(4) : 601-606

[3] J. Marescaux,B. Dallemagne,S. Perretta et al, Surgery without scars: Report of transluminal cholecystectomy in a human being, *Archives of Surgery*, 2007 ,142(9) : 823-826

[4] C.N. Riviere, J. Gangloff, M. De Mathelin, Robotic Compensation of Biological Motion to Enhance Surgical Accuracy *Proceedings of the IEEE*, Volume 94, Issue 9, Sept. 2006 Page(s):1705 - 1716

[5] J. Gangloff, R. Ginhoux, M. de Mathelin, L. Soler, J. Marescaux, Model predictive control for compensation of cyclic organ motions in teleoperated laparoscopic surgery *Control Systems Technology, IEEE Transactions on*, Volume 14, Issue 2, March 2006 Page(s):235 - 246

[6] O. Bebek, M.C. Cavusoglu, Intelligent Control Algorithms for Robotic-Assisted Beating Heart Surgery, *Robotics, IEEE Transactions on*, Volume 23, Issue 3, June 2007 Page(s):468 - 480

[7] G. Tao, P. V. Kokotovic, Adaptive control of systems with backlash, *Automatica*, vol. 29, no. 2, pp. 323-335, 1993

[8] S. Hutchinson, G.D. Hager, P.I. Corke, A tutoriel on visual servo control, *IEEE transactions on robotics and automation* october 1996 12(5) : 651-670

[9] T. Inoue, S. Iwai, M. Nakano, High accuracy control of a proton synchrotron magnet power supply, *Proc. 8th IFAC World Congress*, Part 3, PP. 3137-3142, 1981

[10] M. Tomizuka, T. C. Tsao, and K. Chew, Analysis and Synthesis of Discrete-Time Repetitive Controllers, *American Society of Mechanical Engineers Journal of Dynamic Systems, Measurement, and Control*, 111, 353-358, 1989

[11] D. Comaniciu, V. Ramesh, P. Meer, Kernel-based object tracking, *Pattern Analysis and Machine Intelligence, IEEE Transactions on*, Volume 25, Issue 5, May 2003 Page(s):564 - 577

[12] S. Benhimane, E. Malis, Real-time image-based tracking of planes using efficient second-order minimization, *IEEE/RSJ International Conference on Intelligent Robots Systems*, Sendai, Japan, October 2004